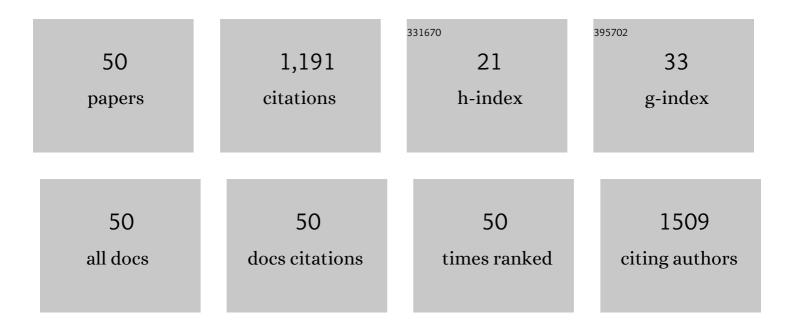
Xue-Min Zhang

List of Publications by Year in descending order

Source: https://exaly.com/author-pdf/6116775/publications.pdf Version: 2024-02-01



#	Article	IF	CITATIONS
1	High-performance plasmonic lab-on-fiber sensing system constructed by universal polymer assisted transfer technique. Nanotechnology, 2022, 33, 095502.	2.6	1
2	Dynamic Color Display with Viewing-Angle Tolerance Based on the Responsive Asymmetric Fabry–Perot Cavity. ACS Applied Materials & Interfaces, 2022, 14, 7200-7207.	8.0	6
3	Controllable Fabrication of PdOâ€PdAu Ternary Hollow Shells: Synergistic Acceleration of H ₂ â€Sensing Speed via Morphology Regulation and Electronic Structure Modulation. Small, 2022, 18, e2106874.	10.0	17
4	Ti3C2 MXene-derived sodium titanate nanoribbons for conductometric hydrogen gas sensors. Sensors and Actuators B: Chemical, 2022, 361, 131693.	7.8	12
5	Pd-decorated PdO nanoparticle nanonetworks: A low-cost eye-readable H2 indicator with reactivation ability. Sensors and Actuators B: Chemical, 2022, 368, 132242.	7.8	8
6	Oriented self-assembly of metal–organic frameworks driven by photoinitiated monomer polymerization. RSC Advances, 2022, 12, 19406-19411.	3.6	4
7	Construction of Zn/Ni Bimetallic Organic Framework Derived ZnO/NiO Heterostructure with Superior <i>N</i> -Propanol Sensing Performance. ACS Applied Materials & Interfaces, 2021, 13, 9206-9215.	8.0	59
8	Self-healing superhydrophobic conductive coatings for self-cleaning and humidity-insensitive hydrogen sensors. Chemical Engineering Journal, 2021, 410, 128353.	12.7	31
9	Preparation of Superhydrophobic Metal–Organic Framework/Polymer Composites as Stable and Efficient Catalysts. ACS Applied Materials & Interfaces, 2021, 13, 32175-32183.	8.0	12
10	Lab-on-fiber sensing system based on responsive Fabry-Perot optical resonance cavities prepared through in-situ construction strategy. Nanotechnology, 2021, 32, .	2.6	1
11	Fabrication of 2D Metal–Organic Framework Nanosheets with Highly Colloidal Stability and High Yield through Coordination Modulation. ACS Applied Materials & Interfaces, 2021, 13, 39755-39762.	8.0	15
12	Green and ultrafast preparation of layered CuO nanoparticles and its ultrahigh-performance ethanol sensing application. Journal of Molecular Liquids, 2021, 342, 117473.	4.9	4
13	A dual-emissive europium-based metal–organic framework for selective and sensitive detection of Fe ³⁺ and Fe ²⁺ . Dalton Transactions, 2021, 50, 13823-13829.	3.3	10
14	Enhancing the Hydrogen-Sensing Performance of p-Type PdO by Modulating the Conduction Model. ACS Applied Materials & Interfaces, 2021, 13, 52754-52764.	8.0	24
15	An ultra-high quantum yield Tb-MOF with phenolic hydroxyl as the recognition group for a highly selective and sensitive detection of Fe ³⁺ . Journal of Materials Chemistry C, 2021, 9, 15840-15847.	5.5	36
16	Sea urchin-like CuO particles prepared using Cu ₃ (PO ₄) ₂ flowers as precursor for high-performance ethanol sensing. Nanotechnology, 2020, 31, 165504.	2.6	11
17	A facile PDMS coating approach to room-temperature gas sensors with high humidity resistance and long-term stability. Sensors and Actuators B: Chemical, 2020, 325, 128810.	7.8	69
18	Solid-state structural transformation of Zn(II)-bpe coordination polymers triggered by dual stimuli. Journal of Solid State Chemistry, 2020, 292, 121635.	2.9	6

XUE-MIN ZHANG

#	Article	IF	CITATIONS
19	Pd-Decorated PdO Hollow Shells: A H ₂ -Sensing System in Which Catalyst Nanoparticle and Semiconductor Support are Interconvertible. ACS Applied Materials & Interfaces, 2020, 12, 42971-42981.	8.0	32
20	Fabrication of wide-detection-range H ₂ sensors with controllable saturation behavior using Au@Pd nanoparticle arrays. Chemical Communications, 2020, 56, 12636-12639.	4.1	12
21	Structural and Morphological Transformation of Two-Dimensional Metal–Organic Frameworks Accompanied by Controlled Preparation Using the Spray Method. Langmuir, 2020, 36, 7392-7399.	3.5	7
22	Copper oxide hierarchical morphology derived from MOF precursors for enhancing ethanol vapor sensing performance. Journal of Materials Chemistry C, 2020, 8, 9671-9677.	5.5	29
23	CoNi-based metal–organic framework nanoarrays supported on carbon cloth as bifunctional electrocatalysts for efficient water-splitting. New Journal of Chemistry, 2020, 44, 1694-1698.	2.8	21
24	MOF-derived CuCoNi trimetallic hybrids as efficient oxygen evolution reaction electrocatalysts. New Journal of Chemistry, 2020, 44, 2459-2464.	2.8	23
25	Encapsulation of metal oxide nanoparticles inside metal-organic frameworks via surfactant-assisted nanoconfined space. Nanotechnology, 2020, 31, 255604.	2.6	5
26	Novel Zinc-Based Infinite Coordination Polymer for Highly Selective Ammonia Gas Sensing at Room Temperature. Bulletin of the Chemical Society of Japan, 2020, 93, 1070-1073.	3.2	11
27	Preparation of hierarchical trimetallic coordination polymer film as efficient electrocatalyst for oxygen evolution reaction. Chemical Communications, 2019, 55, 9343-9346.	4.1	19
28	Fabrication of 2D metal–organic framework nanosheet@fiber composites by spray technique. Chemical Communications, 2019, 55, 8293-8296.	4.1	26
29	Characterization and optimization of the H2 sensing performance of Pd hollow shells. Sensors and Actuators B: Chemical, 2019, 295, 101-109.	7.8	27
30	Amorphous FeNi-bimetallic infinite coordination polymers as advanced electrocatalysts for the oxygen evolution reaction. Chemical Communications, 2019, 55, 12567-12570.	4.1	24
31	The Fabrication of Rigid Crosslinker-Decorated Gold Nanoparticle Array Film for Catalyzing CO2 Cycloaddition. Bulletin of the Chemical Society of Japan, 2019, 92, 2004-2011.	3.2	3
32	Preparation of Bimetallic Metal-Organic Framework Microflowers by Spray Method. Bulletin of the Chemical Society of Japan, 2019, 92, 175-177.	3.2	6
33	Fabrication of MOF Thin Films at Miscible Liquid–Liquid Interface by Spray Method. ACS Applied Materials & Interfaces, 2018, 10, 25960-25966.	8.0	64
34	Fabrication of Metal–Organic Framework and Infinite Coordination Polymer Nanosheets by the Spray Technique. Langmuir, 2017, 33, 1060-1065.	3.5	53
35	Facile fabrication of homogeneous and gradient plasmonic arrays with tunable optical properties via thermally regulated surface charge density. Journal of Materials Chemistry C, 2017, 5, 3962-3972.	5.5	10
36	Optimally designed gold nanorattles with strong built-in hotspots and weak polarization dependence. Nanotechnology, 2017, 28, 495201.	2.6	8

XUE-MIN ZHANG

#	Article	IF	CITATIONS
37	Fabrication of Monodisperse Flower-Like Coordination Polymers (CP) Microparticles by Spray Technique. Nanomaterials, 2017, 7, 237.	4.1	7
38	Metallic Nanoshells with Sub-10 nm Thickness and Their Performance as Surface-Enhanced Spectroscopy Substrate. ACS Applied Materials & amp; Interfaces, 2016, 8, 9889-9896.	8.0	20
39	Modulate the Morphology and Spectroscopic Property of Gold Nanoparticle Arrays by Polymer-Assisted Thermal Treatment. Journal of Physical Chemistry C, 2015, 119, 11839-11845.	3.1	14
40	Optical properties of SiO ₂ @M (M = Au, Pd, Pt) core–shell nanoparticles: material dependence and damping mechanisms. Journal of Materials Chemistry C, 2015, 3, 2282-2290.	5.5	39
41	Highâ€Performance Plasmonic Sensors Based on Twoâ€Dimensional Ag Nanowell Crystals. Advanced Optical Materials, 2014, 2, 779-787.	7.3	40
42	Panchromatic plasmonic color patterns: from embedded Ag nanohole arrays to elevated Ag nanohole arrays. Journal of Materials Chemistry C, 2013, 1, 933-940.	5.5	21
43	Avoiding coffee ring structure based on hydrophobic silicon pillar arrays during single-drop evaporation. Soft Matter, 2012, 8, 10448.	2.7	61
44	Elevated Ag nanohole arrays for high performance plasmonic sensors based on extraordinary optical transmission. Journal of Materials Chemistry, 2012, 22, 8903.	6.7	73
45	Photoinduced cleaning of water-soluble dyes on patterned superhydrophilic/superhydrophobic substrates. Nanoscale, 2010, 2, 277-281.	5.6	21
46	Thermal-induced surface plasmon band shift of gold nanoparticle monolayer: morphology and refractive index sensitivity. Nanotechnology, 2010, 21, 465702.	2.6	44
47	Morphology-controlled two-dimensional elliptical hemisphere arrays fabricated by a colloidal crystal based micromolding method. Journal of Materials Chemistry, 2010, 20, 152-158.	6.7	25
48	Morphology and Wettability Control of Silicon Cone Arrays Using Colloidal Lithography. Langmuir, 2009, 25, 7375-7382.	3.5	103
49	Assembly of non-close-packed 3D colloidal crystals from 2D ones in a polymer matrix viain situ layer-by-layer photopolymerization. Journal of Materials Chemistry, 2008, 18, 3536.	6.7	16
50	UV-Responsive, wide color gamut, inkless dynamic photonic paper enabled by disulfide-containing polyurethane based Fabry-Perot resonant cavity. Journal of Materials Chemistry C, 0, , .	5.5	1